doi: 10.22564/rbgf.v13i2.1190

# SOURCE SIGNATURE DECONVOLUTION OF GROUND PENETRATING RADAR DATA

**Fernando A. Neves[1], Mark S. Roulston[2] & John A. Miller[3]**

Data from a ground penetrating radar (GPR) survey conducted at a site near Cambridge, U.K., were processed. The application of source signature deconvolution using complex spectral division has significantly increased the resolution of the subsurface radar data. The source wavelet was statistically estimated from the radargrams. A velocity structure is suggested, supported by borehole data and analysis of a common mid-point (CMP) gather. A subsurface profile of the area from a 600 m long transect was constructed. This profile showed a clearly defined water table and a gentle rise in an underlying clay layer across the transect.

**Key words:** GPR; Deconvolution; Water table.

**DECONVOLUÇÃO DA ASSINATURA DA FONTE DE DADOS DE RADAR DE PENETRAÇÃO EM SOLO** - *Dados de radar de penetração (RPS) em solo obtidos num levantamento em Cambridge, Inglaterra, foram processados. A aplicação da deconvolução da assinatura da fonte usando divisão espectral complexa aumentou significativamente a resolução dos dados de radar em subsuperfície. A assinatura da fonte foi determinada estatisticamente a partir dos radargramas. Um modelo de velocidade foi então sugerido, baseado em dados de poços e análise de uma família de ponto médio comum (PMC). A partir de uma transecta de 600 m de extensão, um perfil de subsuperfície para a área foi construído. Este perfil mostra uma notável resolução do lençol freático e um suave soerguimento de uma camada de argila ao longo da transecta.*

**Palavras-chave:** *RPS; Deconvolução; Lençol freático.*

[1]Dept. of Earth Sciences, University of Cambridge. Cambridge, CB3 0EZ, England. Also at Depto. de Geofísica-IAG Universidade de São Paulo, Brasil.

[2] Dept. of Physics, Cavendish Laboratories, University of Cambridge.Cambridge, CB3 0HE, England. Now at Division of Geological and Planetary Sciences, California Institute of Technology, Pasadena, CA 91125, USA.

[3]Dept. of Earth Sciences, University of Cambridge. Cambridge, CB3 0EZ, England.

## INTRODUCTION

Ground penetrating radar (GPR) is a surveying method which uses radio waves with frequencies between 1 MHz and 1 GHz to investigate shallow (up to a maximum of 50 m) subsurface features. GPR has been used in a variety of earth science applications including frozen-unfrozen interfaces, mapping soil stratigraphy, subsurface bedrock topography, peat deposits, locating buried pipes and cables, archaeological investigations and measuring the depth to the ground water table (Davis & Annan, 1989; Daniels, 1988). More recently the method has been used in addressing statics problems in reflection seismic data (Fisher et al., 1992).

Reflections from subsurface boundaries are caused by contrasts in the permittivity of different geological materials. Variations in the electrical properties of soils are usually associated with changes in water content. In rock, the propagation of radar waves is sensitive to changes in rock type and the presence of water-filled or dry fractures. Grain size and type can affect the speed of wave propagation in sediments.

Generally, GPR is most effective (greater resolution and depth of penetration) in quartz-rich, dry, clay free sand and gravel. High quality data can also be obtained from similar but water saturated sediments. Muddy sediments containing clay minerals or saline water attenuate the electromagnetic signal owing to high conductivity, which results in limited penetration.

At present much GPR research is concentrated on the development of equipment and software with the aim of bringing it to the level of advance already achieved in seismic exploration. Multichannel receivers and transmitters for collecting spatial GPR data have recently been proposed (Deen & Feijter, 1992).

Research aimed towards the improvement of GPR processing and interpretation includes the introduction of techniques similar to those used in the seismic industry namely : 2-D and 3-D migration (Turner, 1992), complex wavenumber filtering, velocity analysis, forward modelling and deconvolution. All these procedures can help improve geological interpretations made from raw or processed data. Currently, forward modelling is restricted to 1-D structures (Goodman, 1994). Some authors (Todoeschuck et al., 1992; Turner, 1992) have stated that deconvolution of GPR data is not a straight forward procedure and has seldom yielded a great deal of benefit, in that it has given little enhancement in resolution (Annan, 1993). They argue that the radar pulse is often as short and compressed as can be achieved for the given bandwidth and signal-to-noise conditions.

The aim of this paper is to propose a source signature deconvolution using complex spectral division method based upon a statiscally estimated transmitted wavelet derived from the recorded direct wave. This proposed deconvolution was applied to data collected near Cambridge, England (Fig. 1). Since no information about the frequency response of the ground material was available, application of propagation deconvolution which accounts for frequency dependence of attenuation of subsurface radar waves, as proposed by Turner (1994), was not attempted.

## GEOLOGY

The near surface stratigraphy of the area surveyed (Fig. 1), as revealed by the logs of boreholes drilled in 1977, comprises three distinct layers. The soil near the surface is a dark grey sandy or clay loam and is richer in clay lower down. The thickness of the soil is between 0.5 m and 1.0 m. Below the soil is a layer of sandy gravel, forming the second River Terrace of the Cam. The gravel varies from fine to coarse and contains some flint, chalk, sandstone, quartzite and phosphatic nodules. The sand is mainly medium in grain size. Across the section surveyed the thickness of the sandy gravel layer varies from 1.0 m to more than 4.0 m. Below the sandy gravel is Gault clay. The borehole logs show that locally this layer exceeds 3.0 m in thick ness. Chatwin (1975) indicates that it is over 20 m thick in the area surveyed. A summary of the borehole logs marked on Fig. 1 is given in Tab. 1.

| Label | Designation | Elevation | Depths to interfaces | |
|---|---|---|---|---|
| | | | soil/gravel | gravel/clay |
| B1 | TL46 SE102 48576373 | +5.7m | 0.7m | 4.2m |
| B2 | TL46 SE108 49026361 | +4.3m | 0.8m | 1.8m |

**Table 1** - Summary of the borehole logs B1 and B2.
***Tabela 1*** *- Resumo dos perfis de poços B1 e B2.*

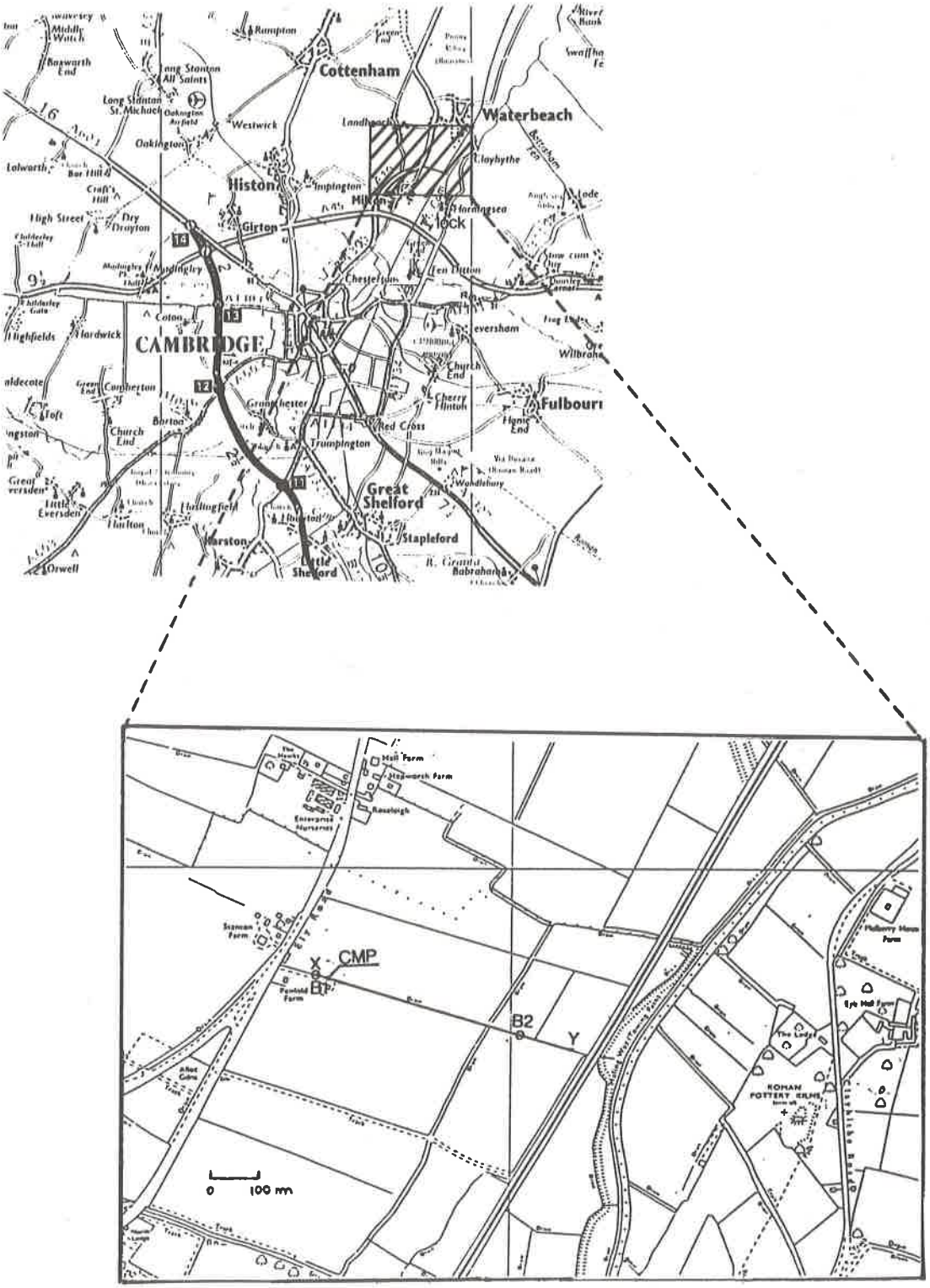


**Figure 1** - Map showing the surveyed area. The shaded area is shown in more detail. The position of Bait's Bite lock, the location of the 600 m transect X-Y , boreholes B1 and B2 and the mid-point of the CMP gather are shown.

***Figura 1*** *- Mapa mostrando a área pesquisada. A área sombreada é apresentada em maior detalhe. A posição da comporta Bait Bite, a localização da transecta X-Y de 600 m, dos poços B1 e B2, e do ponto médio comum da família de PMC são indicados.*

## THE GPR METHOD

### Reflection profiling

Profiling by GPR is similar to sonar and seismic reflection profiling, except that it is based upon the measurement of the travel-time of reflected electromagnetic waves. Davis & Annan (1989) provide a review of GPR principles.

Reflection profiles were produced using a constant separation of 0.5 m between the transmitter and receiver antennae. The antennae were oriented such that the polarization of the signal was perpendicular to the transect line. Recorded traces were obtained every 0.25 m along the length of the profile. The sampling time was 2.4 ns and the total recorded time was 300 ns. A transmitter frequency of 50 MHz was employed in order to investigate variations in stratigraphy, down to the clay layer. The station separation, sampling frequency and total recorded time were chosen using the recommendations on survey design described by Annan (1993).

The 600 m transect made north of a drainage ditch at Penfold Farm is shown as the line X-Y on Fig. 1. The locations of the two boreholes are also shown on Fig. 1. The water level in the drain adjacent to point X was measured as $2.1 \pm 0.1$m relative to the surface of the field. Using the elevation of borehole B1 this corresponded to an elevation of the water level of +3.6 m o.d.. The elevation of the water table at Baits Bite Lock had also been measured as +3.9m o.d..

### Common Mid-point Gathers

Common Mid-point Gather is a standard surveying method used in seismology. The principles involved are almost the same when radar is used. The sampling rate used was the same as for GPR reflection profiling. The transmitter and receiver were initially placed along side each other, at the common mid-point (CMP), then each was moved in opposite directions away from the CMP in steps of 0.1 m. GPR traces were obtained out to a separation of about 10 m. The time window used for the CMP surveying was also 300 ns and the antenna frequency was 50 MHz. The position of the CMP is shown on Fig. 1. Moveout was parallel to the transect line and the polarization of the transmitted radar signal was again perpendicular to the transect line.

## APPARATUS

### Description

The radar system used to obtain the GPR profiles was manufactured by Sensors & Software Inc. and is known as the PulseEKKO™IV. The transmitting and receiving antennae of the system were separable. The transmitted pulse was a wavelet with a nominal frequency of 50 MHz. The pulses were emitted at a frequency of 30 KHz. Each sample was converted into a 16 bit digital number and recorded in a field microcomputer. In order to increase the signal to noise ratio the returns from 256 separate pulses were stacked together to produce each trace recorded.

### Resolution

The GPR horizontal resolution (r) and vertical resolution (vr), assuming that the accuracy of the radar is pulse limited, are given by (Rees, 1977) :

$$r^2 = (D + Vt/2)^2 - D2, \quad (1)$$

$$v_r^2 = Vt/2, \quad (2)$$

where, D is the distance from the radar antennae to the reflecting surface, V the average velocity of the radar pulse and t the pulse duration.

In this model the pulse amplitude over time t is assumed to be constant. However in calculations (section on velocity structure), t has been assumed to be the period of a single cycle at the operating frequency 50 MHz.

## PROCESSING

### Zero-time correction

During the survey the time of arrival of the air wave was seen to drift. In a long reflection profile the arrival time could change by about 20 ns and was corrected by using the arrival time of the direct wave, to redefine the zero-time. All data were corrected in this way. This correction could not be applied to CMP results because in these instances the arrival time of the direct wave increases with antennae separation. However, during a typical CMP survey of about 10 m the zero-time drift was always less than 5 ns, therefore the error introduced was significantly less than the intrinsic vertical resolution given by Eq. (2).

The data was processed and plotted using the commercial software pulseEKKO™IV (version 3.1).

**Gain and filtering**

The adaptive gain automatic gain control (AGC) was applied to the raw data, in an attempt to emphasize reflections and stratigraphic horizon continuity.

The finite sampling frequency of the receiver can introduce low frequency noise into the signal as can inductive effects in the apparatus. Very low frequencies were filtered out of the raw data using the commercial software before further processing. This process in known as *dewowing*.

To remove high frequency noise from the data a 3-point median filter was used. This filter was applied to the raw data using the commercial software to remove frequencies around 210 MHz (Nyquist frequency).

**Source signature deconvolution**

The recorded signal r(t) can be represented as a convolution of the source signal s(t), the response function of the ground g(t) and the response of the receiver h(t):

$$r(t) = s(t)*g(t)*h(t), \quad (3)$$

were $*$ means temporal convolution and t is time.

Fourier transforming Eq. (3) to frequency domain, we obtain:

$$R(f) = S(f)G(f)H(f), \quad (4)$$

were the upper case characters describe the Fourier transforms of the previously defined lower case symbols and f is the temporal frequency.

The main aim of deconvolution is to remove the effect of the source waveform from the recorded data. This process can be represented mathematically by

$$R''(f) = R(f)/S(f) = G(f)H(f). \quad (5)$$

It is well-known that deconvolution is an ill-posed operation, due to the bandlimited nature of the wavelet and the effect of noise. Therefore in order to regularize this operation, we have added a white noise, also called water lever parameter $\mu$. Thus Eq. (5) becomes:

$$R(f) = R(f)*S^*(f)/(S(f)*S^*(f) + \mu) \quad (5a)$$

where $S^*(f)$ is the complex conjugate of S(f). After some test, the value of $\mu$ was set to 1% of the maximum wavelet power.

If an inverse Fourier transform is then performed on R'(f) the deconvolved function r'(t) can be obtained. If it is assumed that the response of the receiver is a constant, say unity, for the dominant frequency components of the recorded signal then

$$r'(t) = g(t), \quad (6)$$

that is, the deconvolved recorded data represents the response function of the ground.

A Fast Fourier Transform (FFT) algorithm was used to perform a Fourier transform on the functions to obtain S(f) and R(f). Eq. (5) was then used to obtain R'(f). An inverse FFT was then performed on R'(f) to obtain r'(t). The theory of FFT and deconvolving algorithms are discussed in Press et al. (1986) from where the necessary subroutines were obtained.

## FIELD DATA

**Reflection profile**

Fig. 2 shows the initial 50m (beginning at point X) of the GPR reflection profile X-Y (Fig. 1). The three uppermost continuous reflectors represent air-wave and ground-wave arrivals and should not be confused with reflections from subsurface interfaces. Interpretation of the whole section was made difficult by the complexity of the source waveform. The reflections are spaced closely in time leading to mixing of the arrivals from different reflectors. The interfaces become more closely spaced towards the eastern end (point Y) of the transect. It was at this stage in the work that we considered that application of source signature deconvolution could help interpretation.

**Velocity structure**

The results of a typical CMP are shown in Fig. 3. The velocity structure was calculated by using $X^2$-$T^2$ graphs. A least-squares fit method was used to obtain the gradient, intercept and scatter of the points from the $X^2$-$T^2$ graphs. An average velocity of $0.07 \pm 0.01$ mns$^{-1}$ was obtained. The time axis intercept corresponds to a depth of $2.0 \pm 0.1$m. The results of other CMPs suggested the same velocity distribution.

Having D = 2.0m, f = 50 MHz (with t = 1/f), Eqs. (1) and (2) give horizontal and vertical resolution of about 1.5m and 0.7m, respectively.

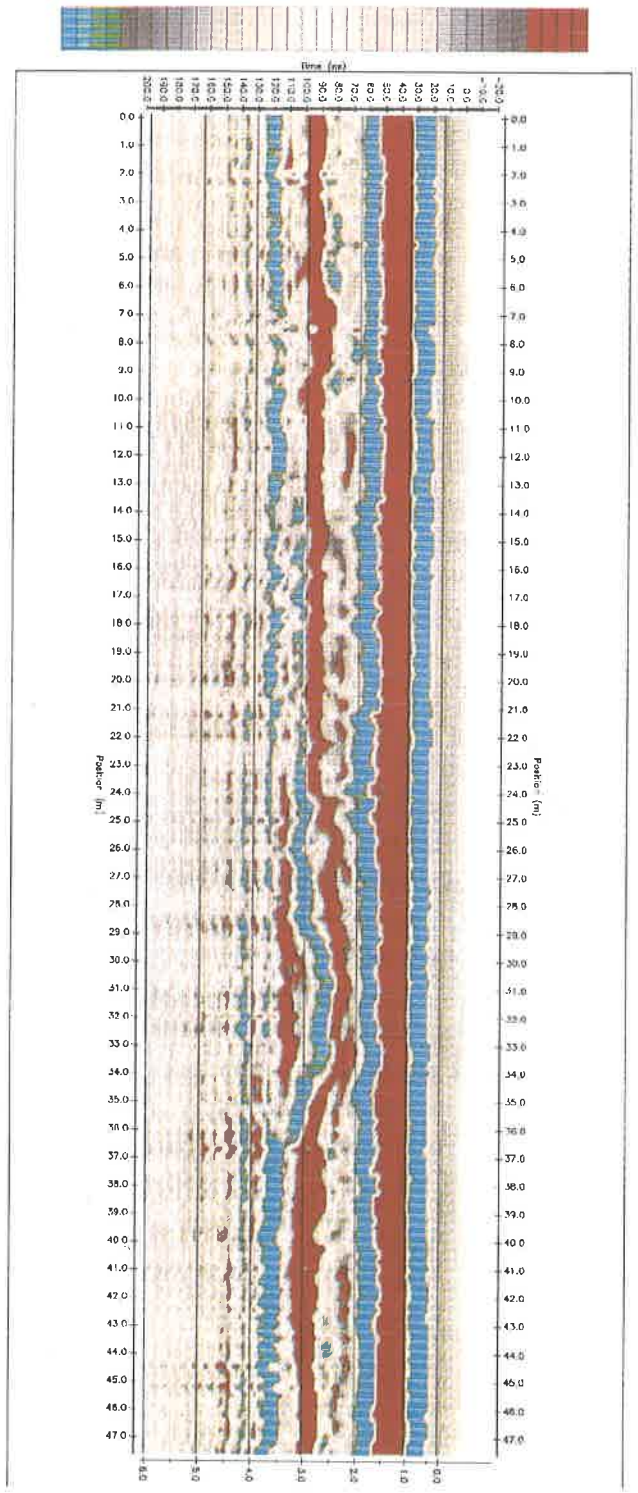

**Figure 2** - The first 50 m (from point X) of the unprocessed X-Y GPR profile (Fig. 1). Note the definition of the reflection from water table at about 95 ns.

***Figura 2*** - *Primeiros 50 m (a partir do ponto X) da seção de RPS não processado do perfil X-Y (Fig. 1). Note a reflexão do lençol freático (em torno de 90 ns tempo de trânsito de ida e volta).*

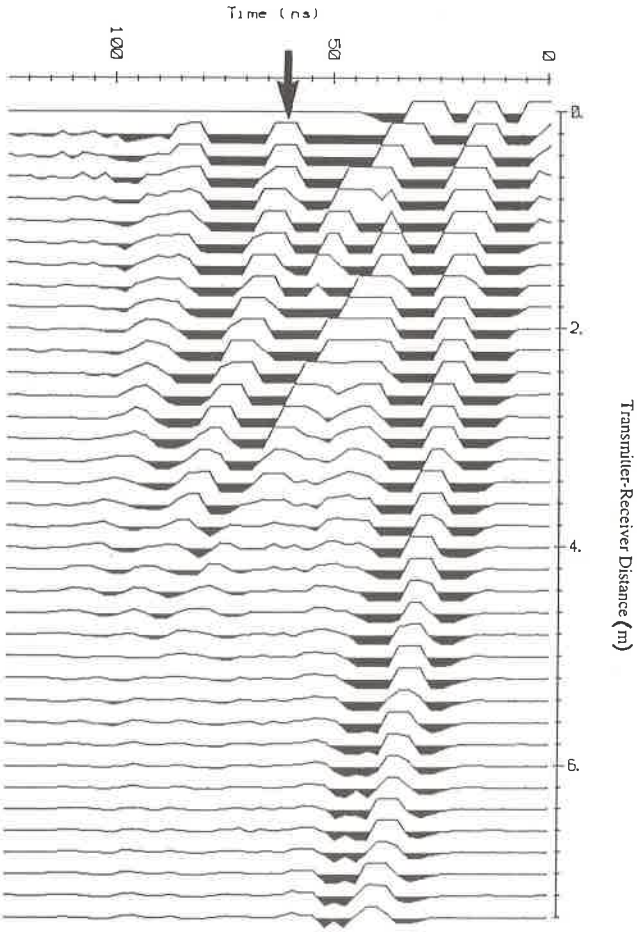


**Figure 3** - A CMP gather from X-Y profile. The reflection used for velocity analysis is marked with an arrow.

***Figura 3*** - *Família de ponto médio comum da linha X-Y. A reflexão usada para análise de velocidade está marcada com uma flexa.*

## DATA PROCESSING AND INTERPRETATION

### Data deconvolution

Our primary goal of applying source signature deconvolution to GPR data was to aid interpretation. Removing the effect of source waveform from the data provided justification for using the value of t=1/f in Eqs. (1) and (2) rather than the duration of the complete source signal.

A typical raw trace (obtained 20m east of point X) is shown in Fig. 4a; its power spectrum is shown in Fig. 4b, to illustrate the effect of source signature deconvolution. This trace was choosen since point X had the highest elevation on the transect and it was assumed, therefore, that the water table would be the deepest resulting in less mixing of the water table reflection with the direct wave.

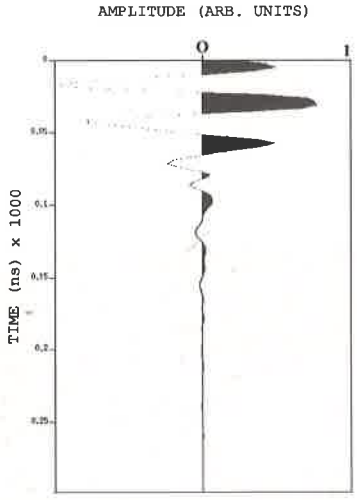


**Figure 4a** - Undeconvolved trace obtained at point X shown in Fig. 1.

***Figura 4a*** - *Traço não deconvolvido obtido no ponto X da Fig. 1.*

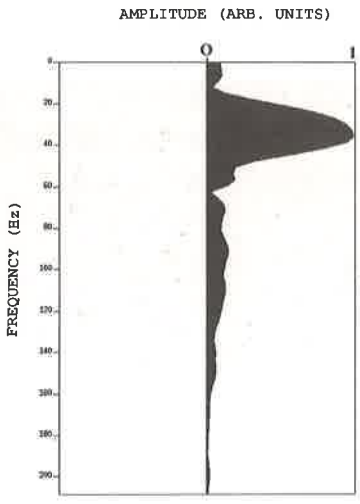


**Figure 4b** - The power spectrum of Fig. 4a.

***Figura 4b*** - *Espectro de potência da Fig. 4a.*

Because the exact source wavelet was not known progress was made by averaging the direct wave which had travelled from transmitter to the receiver for the 2400 raw radar traces. The estimated source signature is shown in Fig. 5a and its power spectrum is given in Fig. 5b. The power spectrum suggested that the dominant frequency component of the source was lower than the nominal frequency of the transmitter, being closer to 35 MHz than 50 MHz. This, however might have been caused by strong frequency dependent attenuation in the near surface soil and/or an effect of the average operation performed to estimate the source signature.

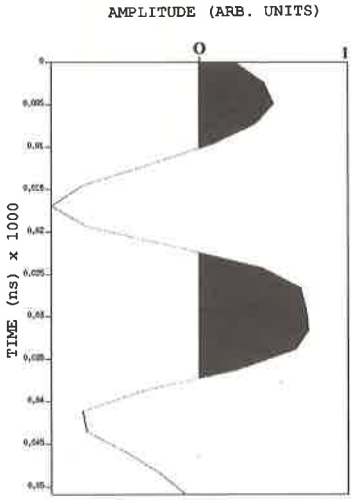


**Figure 5a** - Estimated source signature.

***Figura 5a*** - *Estimativa da assinatura da fonte.*

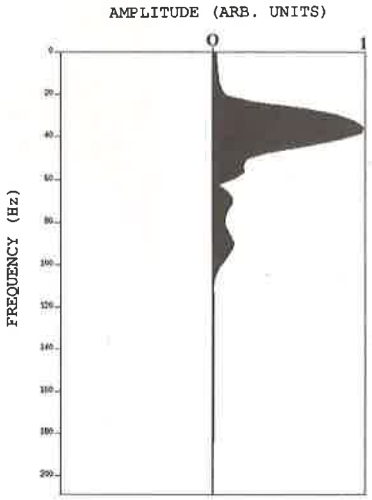


**Figure 5b** - The power spectrum of Fig. 5a.

***Figura 5b*** - *Espectro de potência da Fig. 5a.*

Deconvolution yielded the trace shown in Fig. 6a, which has the power spectrum illustrated in Fig. 6b. Inspection of CMP data such as the one shown in Fig. 3 suggests that Fig. 5a is a good estimation/approximation to the source wave function. Thus all 2400 traces from the transect were deconvolved using this source wave function.

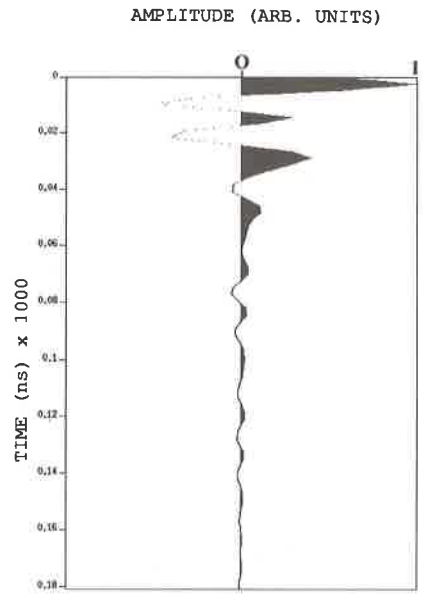


**Figure 6a** - Deconvolved trace of Fig. 4a using the source signature of Fig. 5a.

***Figura 6a*** - *Traço deconvolvido da Fig. 4a usando a assinatura da fonte da Fig. 5a.*

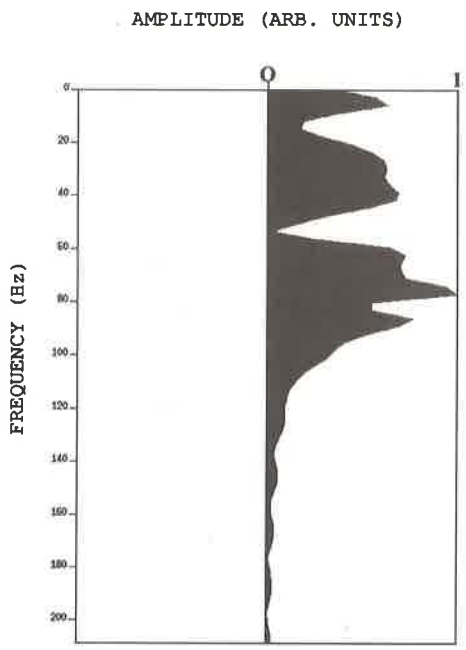


**Figure 6b** - The power spectrum of Fig. 6a.

***Figura 6b*** - *Espectro de potência da Fig. 6a.*

## Data interpretation

The deconvolved section for the 600 m profile X-Y down to 180 ns was plotted and is shown in Fig. 7a. Using the borehole logs and the results of the CMP data, it was inferred that no primary reflections would be present beyond 180 ns, and also from the real trace (Fig.4a). The main reflecting horizons within the section were interpreted and are shown in Fig. 8. For comparison Fig. 7b shows the same section **before** deconvolution. The increase in resolution, from Fig. 7b to Fig. 7a, as a result of our proposed deconvolution is obvious. The clay ridge clearly defined at position 500 m on Fig. 7a can barely be seen in Fig. 7b. The reflection from the water table is patchy throughout the undeconvolved section but it can be traced across the deconvolved section at about 60 ns at position 0 m. Note also that higher frequencies are more dominant above the water table than below it, as would be expected due to the high frequency attenuation of saturated gravel. This effect can only be seen after deconvolution.

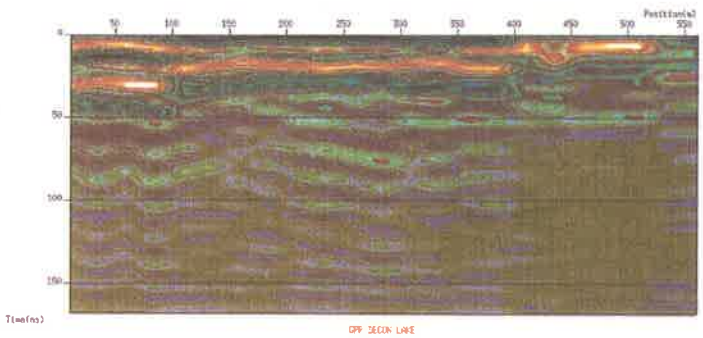

**Figure 7a** - The X-Y radar section deconvolved using the source signature of Fig. 5a.

***Figura 7a*** - *Seção de radar da linha X-Y deconvolvida usando a assinatura da fonte da Fig. 5a.*

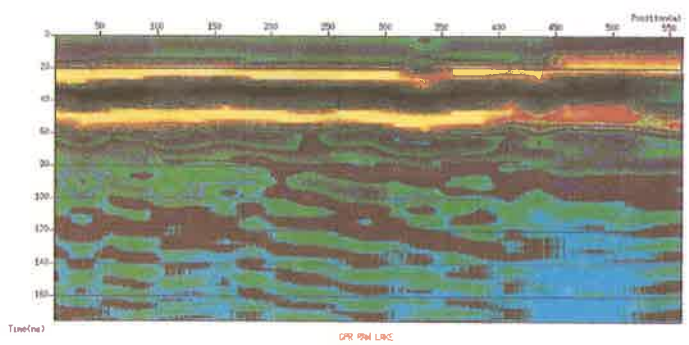

**Figure 7b** - The X-Y radar section before deconvolution.

***Figura 7b*** - *Seção de radar da linha X-Y antes da deconvolução.*

Comparison of Fig. 7a with the borehole logs listed in Tab. 1 and the results from the CMP analysis suggested the interpretation seen in Fig. 8.

Based upon this interpretation, the borehole logs and the CMP results, the velocity in each of the layers was calculated. These are shown in Tab. 2.

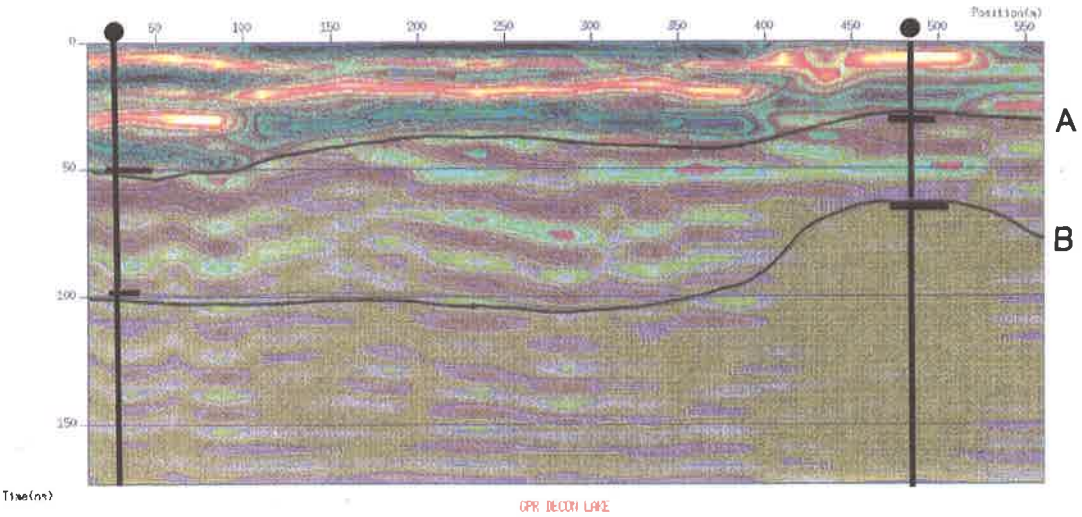


**Figure 8** - Interpretation of the deconvolved radar section of Fig. 7a. A is the primary reflection from the water table and B is the primary reflection from the top of the Gault clay. The location of the two boreholes are shown by vertical solid bars.

***Figura 8*** *- Interpretação da seção de radar deconvolvida da Fig.8a. A é a reflexão primária do lençol freático e B é a reflexão primária do topo da argila Gault. A localização dos poços está mostrada por barras sólidas verticais.*

| Layer | Velocity m/ns |
|---|---|
| Soil | $0.10 \pm 0.01$ |
| "Dry" gravel | $0.07 \pm 0.01$ |
| "Wet" gravel | $0.11 \pm 0.02$ |

**Table 2** - Inferred velocity structure for the profile X-Y
***Tabela 2*** *- Estrutura de velocidade para o perfil X-Y.*

Using the velocities given in Tab. 2, the average velocity down to the water table (2.3 m deep) is 0.08 $mns^{-1}$ which is consistent with the CMP results to within experimental errors. The two-way travel-times were then converted to depths using the velocities given in Tab. 2. The calculated elevations of each of the reflectors is shown in the subsurface profile given in Fig. 9.

## CONCLUSIONS

The main geological-geophysical inferences are summarized in Fig. 9. The most obvious features are the position of the "water table" and the rise of the clay-gravel interface at the eastern end of the transect. These are consistent with the borehole logs and with the geological map for the region (Chatwin, 1975).

In spite of the apparently clear definition of the "water table" in the raw data (Fig. 2) its exact elevation is difficult to ascertain not least due to the problem of defining the water table in terms of its electrical properties. However, the elevation indicated for the water table in Fig. 9 is consistent with the measurements made at the surveyed site.

The interpretation suggests that there is an increase in velocity below the water table. This unexpected result is possibly due to the false assumption that most of the energy of the radar signal is reflected from the top of the water table as defined by hydrology. We suggest that most of the reflected energy comes from a level a few tens of centimetres above the level of the hydrological water table.

Although Annan (1993) asserts that the radar source signature is already so compressed that deconvolution rarely yields any benefit, the results obtained from this study show that source signature deconvolution of GPR data can assist in interpretation. The comparison of Figs. 7a and 7b demonstrates adequately the advantages of deconvolution. Both the top of the Gault clay and the water table are continuously represented only in the deconvolved section. Less noisy results might have been obtained if a better estimate of the source function had been made. We have used the source wavelet obtained from lifting both transmitting and receiving antennae off the ground and recording the direct wave for deconvolution. We have got worser results with this wavelet. We believe this worser results are due to not taking into account the coupling between transmitter/receiver and ground, which is considered when using the direct wave for wavelet

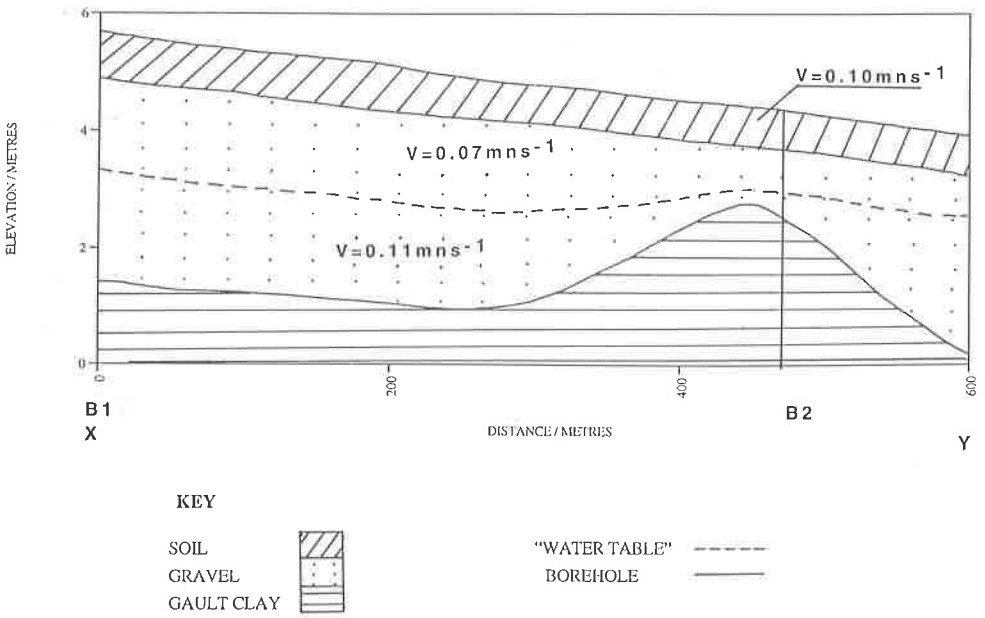


**Figure 9** - Subsurface geophysical-geological model from the X-Y transect line. This profile was constructed using deconvolved GPR data, CMP velocity analysis and borehole logs. The location of the boreholes (B1 and B2) are shown.

***Figura 9*** - *Modelo geofísico-geológico de subsuperfície da transecta X-Y. Este perfil foi construído usando os dados de GPR deconvolvidos, a análise de velocidade da família de PMC e os dados de poços. A localização dos poços (B1 e B2) estão mostrados.*

estimation. It is evident that an accurate estimate of the source function is crucial for the success of source signature deconvolution. And this constitutes an important area of research to be addressed for GPR data processors. Care was taken when applying our processing scheme, but whether some of the results were a manifestation of the processing rather than the signal is not completely certain.

Interpretation of undeconvolved raw data would probably have been easier if a higher frequency signal had been used in the survey. A 100 MHz source being a more time compressed source wavelet would increase data resolution but the penetration of the higher frequency signal would have been less.

## ACKNOWLEDGMENTS

The authors would like to thank Bruce Brisling, Peter Fenning and Jeremy Niblett for their contributions to collecting the data for this research. We appreciate the critical review of this manuscript and instructive comments by two anonymous reviewers. One of us (F. N.) acknowledges a scholarship from the Brazilian Research Council (CNPq) and University of São Paulo. We thank Mr. A. J. Wagstaff of Penfold Farm, Milton, Cambridge, for kindly allowing us access to the site.

## REFERENCES

**ANNAN, A. P. - 1993** - Practical processing of GPR data. Proc. of the Second Government Workshop on Ground Radar, Columbus, Ohio, USA.

**CHATWIN, C. P.- 1975** - British Regional Geology, East Anglia and Adjoining Areas. H.M.S.O..

**DANIELS, J. - 1988** - Locating caves, tunnels and mines. The Leading Edge, **7:** 32-37.

**DAVIS, J. L. & ANNAN, A. P. - 1989** - Ground-penetrating radar for high resolution mapping of soil and rock stratigraphy. Geophysical Prospecting. **37:** 531-551.

**DEEN, J. K. & FEIJTER, J. W. - 1992** - Three-dimensional ground probing radar. Finland Geol. Sur., 4th Intern. Conf. of Ground Penetrating Radar, special paper, **16:** 35-40.

**FISHER, E., McMEHAN, G. A. & ANNAN, A. P. - 1992** - Acquisition and processing of wide-aperture ground penetrating radar data. Geophysics, **57:** 494-504.

**GOODMAN, D. - 1994** - Ground-penetrating radar simulation in engineering and archaeology. Geophysics, **53:** 224-232.

**PRESS, W. H., FLANNERY, B. P., TEUKOLSKY, S. A. & VETTERING, W. T. - 1986** - The Art of Scientific Computing. Cambridge University Press.

**REES, W. G. - 1977** - Physical Principles of Remote Sensing. Cambridge University Press.

**TODOESCHUCK, J. P., LaFLECHE, P. T., JENSEN, O. G., JUDGE, A. S. & PILON, J. A. - 1992** - Deconvolution of ground probing radar data. Geological Survey of Canada, paper **90:** 227-230.

**TURNER, G. - 1992** - Propagation deconvolution. Fourth Inter. Conf. on Ground Penetrating Radar. Geological Survey of Finland, special paper **16:** 85-93.

**TURNER, G. - 1994** - Subsurface radar propagation deconvolution. Geophysics, **59:** 215-223.

Submetido em: 30/05/94
Revisado pelo(s) autor(es) em: 10/02/95
Aceito em: 20/03/95

# DECONVOLUÇÃO DA ASSINATURA DA FONTE DE DADOS DE RADAR DE PENETRAÇÃO EM SOLO

*O uso e a sofisticação de dados de radar de penetração em solo (RPS) aumentou significativamente a partir dos anos 80. Nos últimos 5 anos, o processamento do sinal em formato digital tornou possível aplicar em dados de radar as técnicas comumente usadas em processamento de dados sísmicos. Com efeito, o volume de dados e os resultados das aquisições de RPS aumentaram enormemente. Dentre essas técnicas, abordamos neste artigo a deconvolução da assinatura da fonte usando divisão espectral complexa. O objetivo do processo de deconvolução é comprimir a assinatura da fonte e assim aumentar a resolução dos dados.*

*Os dados de RPS usados neste artigo foram obtidos num levantamento executado nos arredores da cidade de Cambridge, na Inglaterra. Uma vez que o volume de dados obtidos num levantamento de RPS é relativamente pequeno, quando comparado com o obtido num levantamento sísmico convencional, e que a velocidade de aquisição é também maior, um pré-processamento ainda na área de aquisição é factível. O sistema de aquisição usado foi o PulseEKKO IV. As antenas foram orientadas perpendicularmente à direção de aquisição. A freqüência dominante da antena transmissora foi de 50 MHz e a razão de amostragem foi de 2.4s, com cobertura nominal vertical de 256.*

*O pré-processamento dos dados englobou as correções estáticas de campo devido à variação da topografia e à deriva do tempo-zero. A deriva do tempo-zero é corrigida determinando-se o tempo-zero para cada pulso de radar, a partir da onda aérea direta. Afim de restaurar as amplitudes verdadeiras dos dados, a correção do espalhamento geométrico e da atenuação foi efetuada. A seguir, filtragem no domínio da freqüência e ganhos do tipo CGA (Controle de Ganho Automático) foram aplicados. Com esta fase almejou-se ressaltar específicos refletores de interesse, observados na seção de radar. Após esta fase nos pareceu necessária e óbvia a tentativa de se aplicar a deconvolução, uma vez que a baixa resolução dos dados não permitia a distinção/identificação dos refletores no radargrama.*

*A aplicação da deconvolução da assinatura da fonte aumentou significativamente a resolução dos dados de radar em subsuperfície. A assinatura da fonte foi determinada estatisticamente a partir dos radargramas. Uma pequena porcentagem de ruído branco (1%) foi adicionada aos dados afim de regularizar o processo de deconvolução.*

*Adiante, um modelo de velocidade foi então sugerido, baseado em dados de poços e análise de uma família de ponto médio comum (PMC). A partir de uma transecta de 600 metros de extensão, um perfil de subsuperfície para a área foi construído. Este perfil mostra uma notável resolução do lençol freático e um suave soerguimento de uma camada de argila ao longo da transecta. Por outro lado, apesar desta clara identificação do lençol freático, a definição em profundidade deste refletor é problemática de se estimar, posto que a premissa de que grande parte ou a maior parte da energia é refletida no topo do lençol, nos parece incorreta, posto que um aumento de velocidade abaixo do lençol freático foi observado.*